



Vortex creep down to 0.3 K in superconducting Fe(Te,Se) single crystals

Thierry Klein, Hadrien Grasland, Hervé Cercellier, Pierre Toulemonde, C. Marcenat

► To cite this version:

Thierry Klein, Hadrien Grasland, Hervé Cercellier, Pierre Toulemonde, C. Marcenat. Vortex creep down to 0.3 K in superconducting Fe(Te,Se) single crystals. *Physical Review B: Condensed Matter and Materials Physics* (1998-2015), 2014, 89 (1), pp.014514. 10.1103/PhysRevB.89.014514 . hal-00956263

HAL Id: hal-00956263

<https://hal.science/hal-00956263>

Submitted on 6 Mar 2014

HAL is a multi-disciplinary open access archive for the deposit and dissemination of scientific research documents, whether they are published or not. The documents may come from teaching and research institutions in France or abroad, or from public or private research centers.

L'archive ouverte pluridisciplinaire **HAL**, est destinée au dépôt et à la diffusion de documents scientifiques de niveau recherche, publiés ou non, émanant des établissements d'enseignement et de recherche français ou étrangers, des laboratoires publics ou privés.

Vortex creep down to 0.3 K in superconducting Fe(Te,Se) single crystals

T. Klein,¹ H. Grasland,¹ H. Cercellier,¹ P. Toulemonde,¹ and C. Marcenat²

¹Université de Grenoble-Alpes, Inst NEEL, F-38042 Grenoble, France and CNRS, Inst NEEL, F-38042 Grenoble, France

²SPSMS, UMR-E9001, CEA-INAC/ UJF-Grenoble 1, 17 Rue des Martyrs, 38054 Grenoble, France

(Received 21 November 2013; revised manuscript received 8 January 2014; published 29 January 2014)

We report on a study of the vortex creep in $\text{Fe}_{1+\delta}(\text{Te}_x\text{Se}_{1-x})$ single crystals ($x = 0.5$ and 0.4) down to 0.28 K ($\sim T_c/50$) and up to $\mu_0 H_a = 2$ T. The relaxation of the current density $[J(t)]$ has been measured during 20 hours and the decay of $J(t)$ can be well described by a $J(t) \propto [\ln(t/t_0)]^{-1/\mu}$ law. We show that the relaxation exponent μ tends towards 0 for $T < 2$ K and $\mu_0 H_a < 0.1$ T [i.e. $J(t) \rightarrow (t_0/t)^\alpha$] and increases for increasing T and/or H_a . Our measurements strongly suggest that the logarithmic creep rate $R = -d \ln(J)/d \ln(t)$ remains finite at zero temperature ($R|_{T \rightarrow 0} \rightarrow 2\%$) and hence that quantum creep plays a dominant role in the relaxation process at low temperature. A maximum is observed in both the temperature and field dependence of $R(t = 100\text{s}, T, H_a)$, which can be associated to a crossover from a single vortex (one-dimensional) to a bundle (three-dimensional) creep regime.

DOI: 10.1103/PhysRevB.89.014514

PACS number(s): 74.25.Wx, 74.70.Xa

I. INTRODUCTION

Iron selenium belongs to the family of iron-based superconductors that has been discovered recently [1]. It has been reported to be superconducting at a critical temperature, T_c on the order of 8 K [2], rising up to ~ 14 K in $\text{Fe}_{1+\delta}(\text{Te}_x\text{Se}_{1-x})$ [3] (for $x \sim 0.5$). This binary compound then shares the most salient characteristics of iron-based pnictides (square-planar lattice of Fe with tetrahedral coordination) without having the structural complexity associated to the presence of a charge reservoir. Specific heat measurements have shown that the coherence length is very small [4]: $\xi_c(0) = \epsilon \xi_{ab}(0) \sim 3.5$ Å (ϵ being the anisotropy parameter $\sim 1/4$), confirming the strong renormalization of the Fermi velocity previously observed by ARPES measurements [5].

On the other hand, the penetration depth is large: $\lambda_c(0) = \lambda_{ab}(0)/\epsilon \sim 1600$ nm [4], so that the condensation energy, $\epsilon \epsilon_0 \xi_{ab} = (1/4)(\Phi_0/8\pi \lambda_{ab})^2 \xi_{ab}$, is small (~ 30 K) and the Ginzburg number $\text{Gi} = (1/8)(T_c/\epsilon \epsilon_0 \xi_{ab})^2 \sim 3 \times 10^{-2}$ is on the order of that previously observed in high- T_c cuprates. As a consequence, thermal fluctuations are large [6] and the pinning energy $U_c \sim T_c/\sqrt{\text{Gi}}(J_c/J_0)^{1/2}$ is very small [~ 10 K, J_c and J_0 being the critical and depairing currents, respectively with $J_c(0) \sim 2 \cdot 10^5$ A/cm² $\sim J_0(0)/100$]. As expected, large flux creep has been observed in $\text{Fe}_{1+\delta}(\text{Te}_x\text{Se}_{1-x})$ [7] (as well as in other iron based compounds [8]), compromising the study of the temperature and field dependence of the critical current. Indeed, despite its much lower T_c value, the logarithmic creep rate of the sustainable current density J , $R = -d \ln(J)/d \ln(t) \sim 2\text{--}6\%$ is again similar to the one previously observed in high-temperature superconductors [9].

At low temperature thermally activated creep is expected to vanish linearly with decreasing temperature ($R|_{T \rightarrow 0}^{\text{th}} \sim kT/U_c$) but it has been observed in several systems [10] (including high- T_c oxides, Chevrel phases, heavy fermions, or organic superconductors), that the relaxation rate does not extrapolate to zero for $T \rightarrow 0$ suggesting a decay of the critical state by quantum tunneling [11]. A similar study in iron-based superconductors was still lacking.

We report here on a detailed study of the vortex creep in $\text{Fe}_{1+\delta}(\text{Te}_x\text{Se}_{1-x})$ single crystals ($x = 0.5$ and 0.4) down to 0.28 K $\sim T_c/50$ (and up to $H = 2$ T). The relaxation has been

recorded on a large time range (up to 20 hours $\equiv 7 \times 10^4$ s), which enabled a clear determination of the relaxation exponent μ . We show that $\mu \rightarrow 0$ for $T < 2$ K (and $\mu_0 H_a < 0.1$ T) and increases for increasing T (and/or H_a). Our measurements strongly suggest that R remains finite at zero temperature with $R|_{T \rightarrow 0} \sim 2\%$ and hence that quantum creep plays a dominant role in the relaxation process at low temperature. We show that the sustainable current density $[J(t)]$ is substantially smaller than J_c and its temperature and/or magnetic field dependence is significantly different from that of J_c . All measurements suggest the existence of a crossover from a single vortex [one-dimensional (1D)] to a bundle (3D) creep regime.

II. SAMPLE AND EXPERIMENTS

The measurements have been performed on $\text{Fe}_{1+\delta}(\text{Te}_x\text{Se}_{1-x})$ single crystals with $x = 0.5$ (sample A) and $x = 0.4$ (sample B). The samples were prepared from very pure iron and tellurium pieces and selenium shots in a 1 : 1 - x : x ratio, loaded together in a quartz tube that has been sealed under vacuum. The elements were heated slowly (100°C/h) at 500°C for 10 h, then melted at 1000°C for 20 h, cooled slowly down to 350°C at 5°C/h , and finally cooled faster by switching off the furnace. Single crystals of typical size $500 \times 500 \times 50$ μm^3 have been mechanically extracted from the resulting ball. Two series of samples with $T_c \sim 14$ K (sample A) and $T_c \sim 10$ K (sample B) have been measured. Both series present well-defined superconducting transitions in AC susceptibility measurements and the reduced T_c in sample B is most probably due to a slightly higher δ value. Batch A has been previously studied into detail using both specific heat and magnetic measurements [4].

The distribution of the magnetic induction perpendicular to the sample surface (a - b plane) has been measured by scanning a miniature GaAs-based quantum well Hall sensor over the sample surface. A typical field contour plot obtained after cycling the field up to 500 G ($H_a \parallel c$) and back to zero is displayed in Fig. 1(a) (sample A, $T = 5.5$ K), clearly showing the good homogeneity of the sample. The field distribution clearly displays a sand-hill shape [see Fig. 1(b)] characteristic of bulk pinning and, correspondingly a V-shape profile is

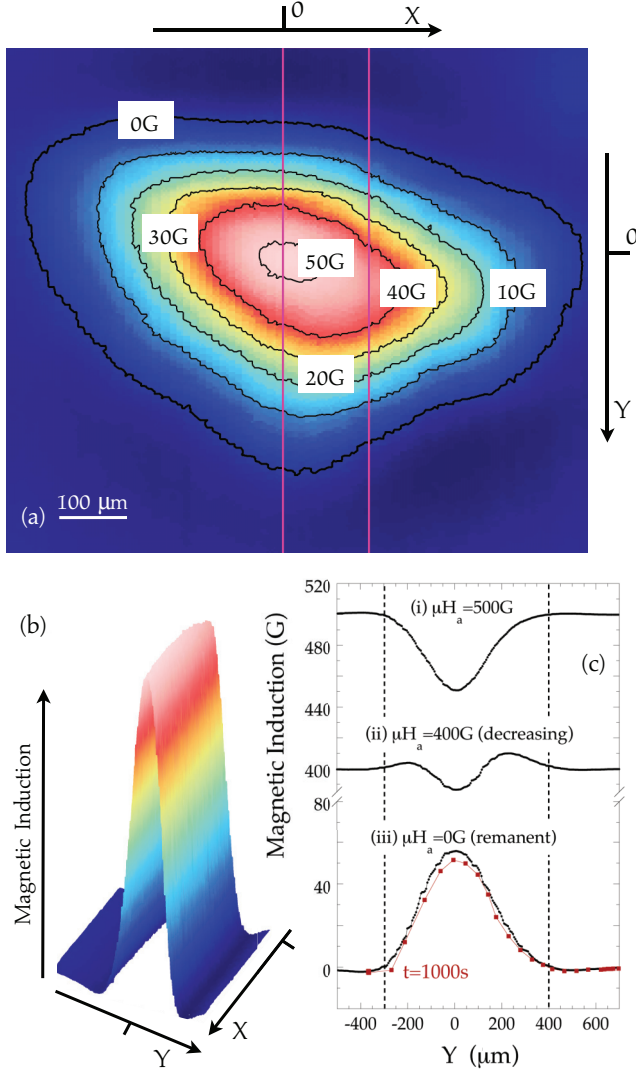


FIG. 1. (Color online) (a) Contour plot of the magnetic induction perpendicular to the sample surface obtained after cycling the field up to 500 G ($H_a \parallel c$) and back to zero (sample A). As shown in (b) the field profile in the purple rectangle clearly displays a sand-hill shape characteristic of bulk pinning. Correspondingly a V-shape profile is obtained for increasing field [see curve (i) at 500 G in (c)] and the profile is progressively reversed as the field is decreased [see curve (ii) and (iii) for $H_a = 400$ G and 0 G, respectively]. The solid (red) symbols for $H_a = 0$ have been recorded after a 1000 s waiting time, clearly showing the decay of the trapped sand hill with time (sample edges are indicated by vertical dotted lines).

obtained for increasing field [see curve (i) at 500 G in Fig. 1(c)]. The solid (red) symbols for $H_a = 0$ were obtained after a 1000 s waiting time, clearly showing the decay of the trapped sand hill with time. The induction gradient obtained by placing an array of ten miniature GaAs-based quantum well Hall sensors right on the sample surface reached $dB/dx \sim 5$ G/ μ m at 4.2 K [i.e., ~ 10 times larger than the one observed during the scans, see Fig. 1(c)] and even ~ 30 G/ μ m at 0.3 K. For a given H_a value, the induction at the center of the sample (B^{up}) has been recorded as a function of time after ramping the field up to H_a starting for a field value much smaller than H_a . Similarly,

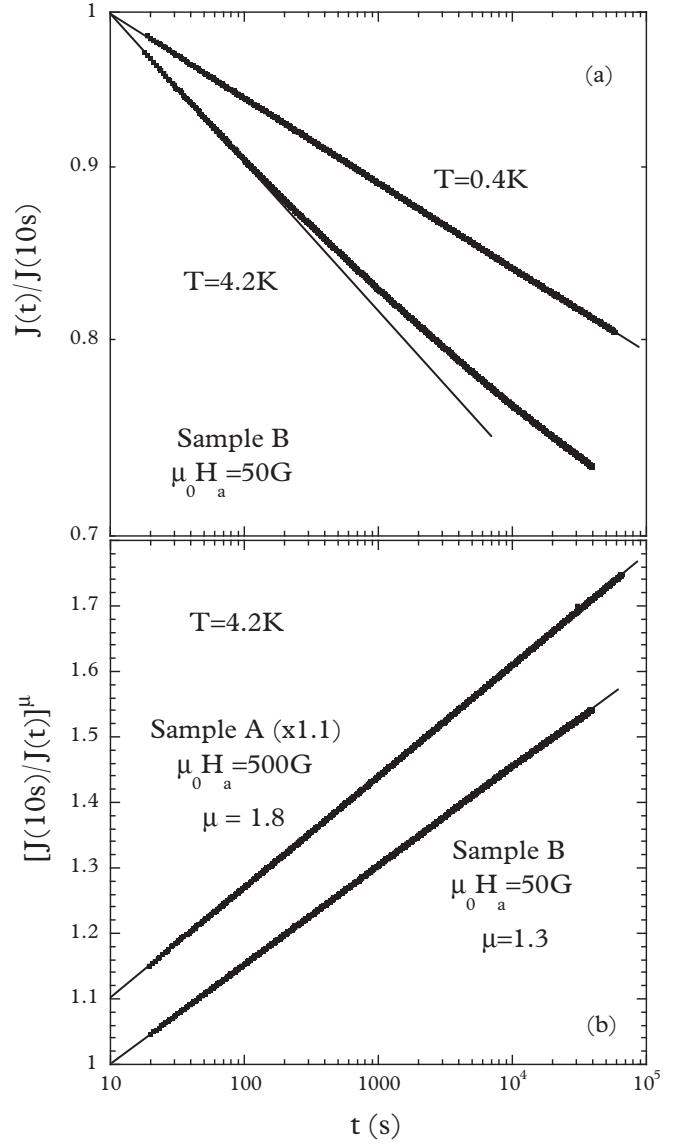


FIG. 2. (a) Time dependence of the normalized sustainable current density (in a log-log scale) up to 20 hours (7×10^4 s) at the indicated temperatures ($\mu_0 H_a = 50$ G) in $\text{Fe}_{1+\delta}(\text{Te}_x\text{Se}_{1-x})$ single crystals. As shown, the time dependence is algebraic at low temperature (0.4 K) but a clear deviation from this algebraic dependence is visible at 4.2 K. (b) As expected from the elastic collective pinning model, this deviation can be well described by a $1/J^\mu \propto \ln(t)$ law (see text for details).

the decay of B^{down} has been recorded after ramping the field down to H_a starting from a field value much larger than H_a . The data acquisition has been started after five seconds to allow for the settling of the field and $J(t)$ has been defined as $J(t) \propto [B^{\text{down}}(t) - B^{\text{up}}(t)]/2$. Figure 2(a) displays the decay of J for $T = 4.2$ K and $T = 0.4$ K (Sample B). All the effects discussed below have been observed in both samples. As shown, at low temperature (typically $T < 2$ K) and low field (typically $\mu_0 H_a < 0.1$ T), $J(t)$ can be very well described by an algebraic law: $J(t) \propto 1/t^\alpha$ with $\alpha \sim 2\%$ for $T \rightarrow 0$. Clear deviations from this algebraic decay become visible above ~ 2 K (and/or for $\mu_0 H_a > 0.1$ T) and, as shown on Fig. 2(b),

$1/J^\mu$ then varies as $\ln(t)$ where the relaxation exponent μ is both temperature and field dependent (see discussion below).

III. DISCUSSION

A. Creeping models

The decay of the sustainable current density with time is determined by the current dependence of the activation barriers. In the case of thermally activated elastic collective creep, this energy is expected to diverge at low J as:

$$U(J) = \frac{U_c \times [(J_c/J)^\mu - 1]}{|\mu|}, \quad (1)$$

where the value of the relaxation exponent μ depends on the dimensionality of the creeping object: $\mu = 1/7$ for single one-dimensional (1D) vortex lines, and $\mu = 5/2$ (7/9) for small (large) 3D vortex bundles. Writing [12] $U(J) = kT \ln(t/t_0)$ for $t \gg \tau$ where τ is a characteristic time related to the transients at the onset of relaxation, one expects:

$$J(t) = \frac{J_c}{[1 + (\mu kT/U_c) \times \ln(t/t_0)]^{1/\mu}} \quad (2)$$

and correspondingly the logarithmic creep rate of the sustainable current density $R = d \ln(J)/d \ln(t)$ is equal to:

$$R^{th}(T) = \frac{1}{U_c/kT + \mu \ln(t/t_0)}, \quad (3)$$

where t_0 is a macroscopic time related to the sample dimensions (and barrier magnitude) $t_0 \sim 10^{-6} - 1$ s (see Ref. [13] and references therein).

On the other hand, the barriers are expected to remain finite for $J \rightarrow 0$ in the case of plastic creep [14]. The $U(J)$ dependence is then expected to be of the same form as that predicted by the theory of thermally activated motion of dislocations in crystalline solids, which can be well approximated by inserting a negative μ values in Eq. (1). The Kim-Anderson model [15] is also reproduced for $\mu = -1$. Finally, it has been suggested by Zeldov *et al.* [16] that barriers could diverge logarithmically:

$$U(J) = U_c \times \ln(J_c/J) \quad (4)$$

[corresponding to $\mu \rightarrow 0$ in Eq. (1)], which is then expected to give rise to an algebraic decay of the current density [17]:

$$J = \frac{J_c}{(t/t_0)^{kT/U_c}} \quad (5)$$

and the relaxation rate is then time independent:

$$R^{th}(T) = kT/U_c \quad (6)$$

In the case of quantum creep, the tunneling rate, $R_{|T \rightarrow 0}^{Qu}$, is determined by the effective Euclidean action [11]: $R_{|T \rightarrow 0}^{Qu} \sim \hbar/S_Q^{\text{eff}} \sim \hbar/U_c t_c$, where t_c is the tunneling time. In the commonly observed limit of strong dissipation for which the dominant term of the equation of motion is the dissipative term, $t_c \sim \eta L_c^2 / \epsilon^2 \epsilon_0$ [13] where $L_c = \epsilon \xi_{ab} (J_0/J_c)^{0.5}$ is the collective pinning length and $\eta = (\xi_{ab} \hbar)^2 / e^2 \rho_n$ the Bardeen-Stephen viscous drag coefficient (ρ_n being the normal-state resistivity). One hence finally expects: $R_{|T \rightarrow 0}^{Qu} \sim (e^2 \rho_n / \epsilon \xi_{ab} \hbar) (J_c/J_0)^{0.5}$ for $J \sim J_c$ and samples with large normal-state resistivities

and small coherence lengths can be considered as good candidates for the observation of quantum creep. Taking $\rho_n \sim 1 \text{ m}\Omega\text{cm}$ [18], $\xi_{ab} \sim 15 \text{ \AA}$, $\epsilon \sim 1/4$ [4], $J_0(0) \sim 3 \times 10^7 \text{ A/cm}^2$ and $J_c(0) \sim J(0, t = 1 \text{ s}) \sim 1/\mu_0 \times dB/dx \sim 2 \times 10^5 \text{ A/cm}^2$ one obtains $\hbar/S_Q^{\text{eff}} = (e^2 \rho_n / \epsilon \xi_{ab} \hbar) (J_c/J_0)^{0.5} \sim 0.1$ indicating that quantum creep can be large in $\text{Fe}_{1+\delta}(\text{Te}_x\text{Se}_{1-x})$. On the other hand, the pinning energy is very small ($\sim 10 \text{ K}$ for $J_c \sim J_0/100$) and the ratio between the classical and quantum rates $[kT/U_c]/[\hbar/S_Q^{\text{eff}}] \sim [T/100] \times [J_0/J_c]$ so that quantum and classical creep are expected to be on the same order of magnitude for $T \sim 1 \text{ K}$.

As for the pinning barriers in the case of classical creep [Eq. (1)], the Euclidian action is expected to diverge for $J \ll J_c$ [$S(J) \propto 1/J^{\mu_s}$ with $\mu_s = \mu + 1$], and very similar expressions are obtained for both classical and quantum creep substituting U_c/kT by S_Q^{eff}/\hbar and μ by μ_s [11] leading to:

$$R_{|T \rightarrow 0}^{Qu} = \frac{1}{S_Q^{\text{eff}}/\hbar + \mu_s \ln(t/t_0)} \quad (7)$$

[see Eq. (3) in comparison]. Note that, as for classical creep, a logarithmic divergence of the Euclidian action would lead to a time-independent $R_{|T \rightarrow 0}^{Qu} = \hbar/S_Q^{\text{eff}}$ value. Finally, at finite temperature, quantum tunneling can be thermally assisted and one finally obtains:

$$R^{Qu}(T) = R^{Qu}(0) \times [1 + (T/T_0)^2] \quad (8)$$

where the characteristic temperature T_0 is related to the microscopic parameters of the dynamical equation [11]. T_0 also marks the crossover from the quantum to the classical creep regime and is hence expected to be on the order of 1 K in our system (see above).

B. Temperature and field dependence of the relaxation rate

For low magnetic fields, the relaxation rate is field independent (see below) and $R(T, t = 100 \text{ s})$ first increases with T , then decreases for $T > T_{\text{max}} \sim (0.2 - 0.3) \times T_c$ and finally rises again as T tends towards the irreversibility line [being close to T_c for the small H_a values used here, see Fig. 3(a)]. Very similar behaviors were obtained in both samples and, as shown, T_{max}/T_c slightly decreases with H_a . Note that even though identical $R(T, t = 100 \text{ s})$ values are obtained for different temperatures ($R(T, t = 100 \text{ s}) \sim 3\%$ for $T/T_c \sim 0.1$, ~ 0.5 and ~ 0.8 for instance), those values correspond to very different creeping regimes (see discussion below).

Indeed, for $T \leq 2 \text{ K}$ (and $\mu_0 H_a \leq 0.1 \text{ T}$) $1/R(T, t)$ is time independent [see Fig. 3(b)] indicating that $U(J)$ [or equivalently $S(J)$ for quantum creep] is diverging logarithmically with J in this temperature (and field) range [Eqs. (4)–(6)], correspondingly, as shown in Fig. 2(a), $J(t) \propto 1/t^\alpha$ with $\alpha = R$. As R remains finite down to the lowest temperature ($\sim 2\%$ for $T \rightarrow 0$) whereas $R^{th}(T) = kT/U_c$ is expected to vanish for T tending towards zero, our data are clearly indicating that the relaxation is dominated by quantum creep at low temperature. Note that, $R(T)$ can be well fitted by a $1 + (T/T_0)^2$ law with $T_0 \sim 2 \text{ K}$ [thick solid line in Fig. 3(a)], in good agreement with the thermally assisted quantum creep scenario [Eq. (8)]. However, our data show that the relaxation process can not be described by the *elastic* collective creep scenario for which μ_s is expected to be significantly different from

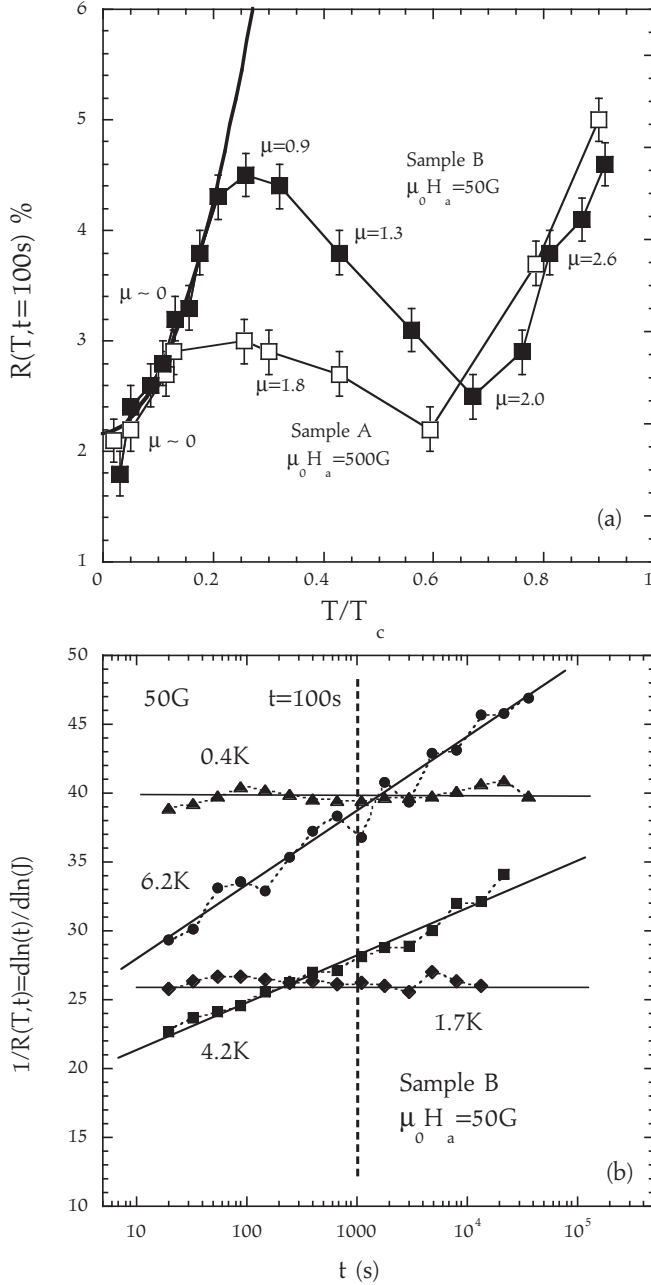


FIG. 3. (a) Temperature dependence of the logarithmic relaxation rate $R = -d \ln(J)/d \ln(t)$ at $t = 100s$ for the indicated field values in sample A ($T_c \sim 14$ K, open squares) and sample B ($T_c \sim 10$ K, solid squares). Thin lines are guides to the eyes and the thick solid line is a $R(0) \times [1 + (T/T_0)^2]$ fit to the data (see text for details). Relaxation exponent (μ) values are indicated for some characteristic temperatures, note that μ rapidly increases above the $R(T)$ peak. (b) $1/R$ as a function of t (Sample B, $\mu_0 H_a = 50$ G) for the indicated T values. As shown the slope of the curve (i.e. μ) is close to 0 below ~ 2 K and increases at higher temperatures (see text for details).

zero ($\mu_s = 8/7$ for single vortices and even larger in the bundle regime) and the nature of the microscopic mechanism leading to a logarithmic divergence of $S(J)$ still has to be elucidated.

As shown in Figs. 3(a)–3(b), a clear change in the relaxation process occurs around T_0 . Indeed for $T > T_0$ $R(T, t = 100s)$ decreases and concomitantly $1/R(T, t)$ is no longer time

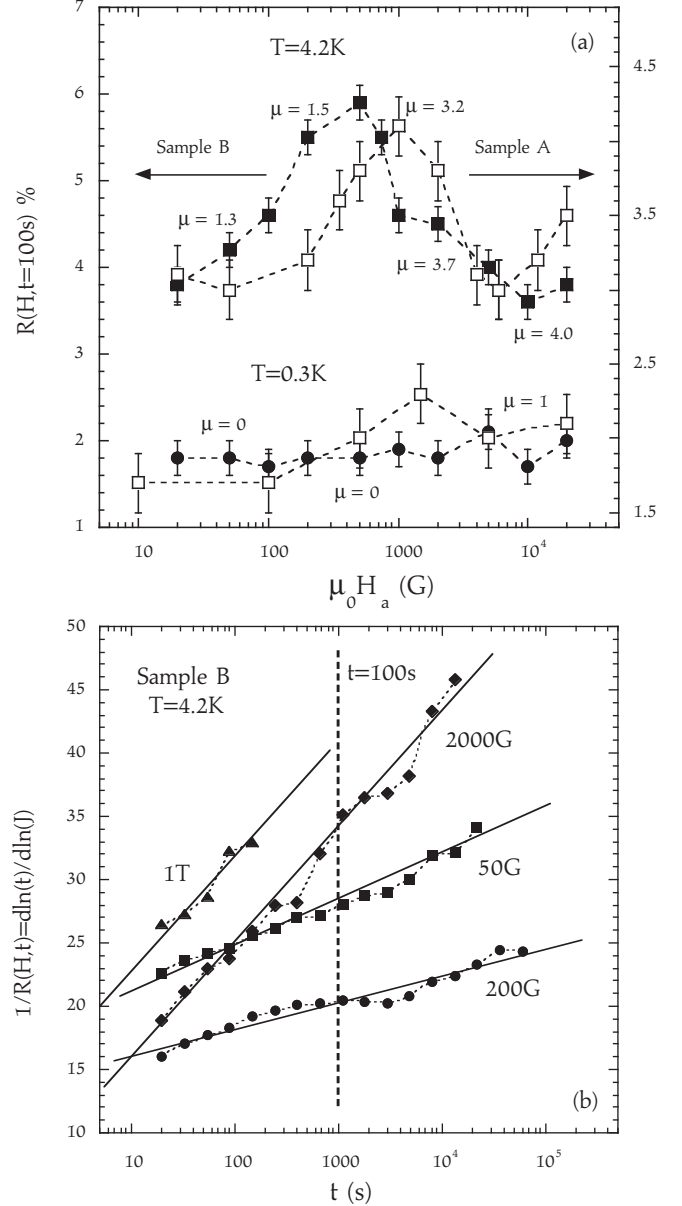


FIG. 4. (a) Magnetic field dependence of the logarithmic relaxation rate $R = d \ln(J)/d \ln(t)$ at $t = 100s$ for the indicated T values in sample A (open squares, right scale) and sample B (solid symbols, left scale). Relaxation exponent (μ) values are indicated for some characteristic fields, note that μ rapidly increases above the $R(H)$ peak. The dotted lines are guides to the eyes. (b) $1/R$ as a function of t (Sample B, $T = 4.2$ K) for the indicated H_a values. As shown the slope of the curve (μ) increases at high fields (see text for details).

independent but varies linearly with $M(t)$. This logarithmic variation is then characteristic of a $1/J^\mu$ divergence of the activation barriers [Eq. (3)] [19]. The decrease of $R(T, t = 100s)$ above T_0 is hence a direct consequence of an increase of the relaxation exponent μ . Similarly, $R(H_a, t = 100s)$ also presents a clear maximum for $\mu_0 H_a (= \mu_0 H_{\max}) \sim 500 - 1000$ G at 4.2 K [see Fig. 4(a)]. At low field μ is constant (~ 1.3 at 4.2K) and $R(H_a, t = 100s)$ increases due to a decrease of the pinning energy with H_a but, as observed for $R(T)$, $R(H_a, t = 100s)$ rapidly decreases above H_{\max} due, again, to

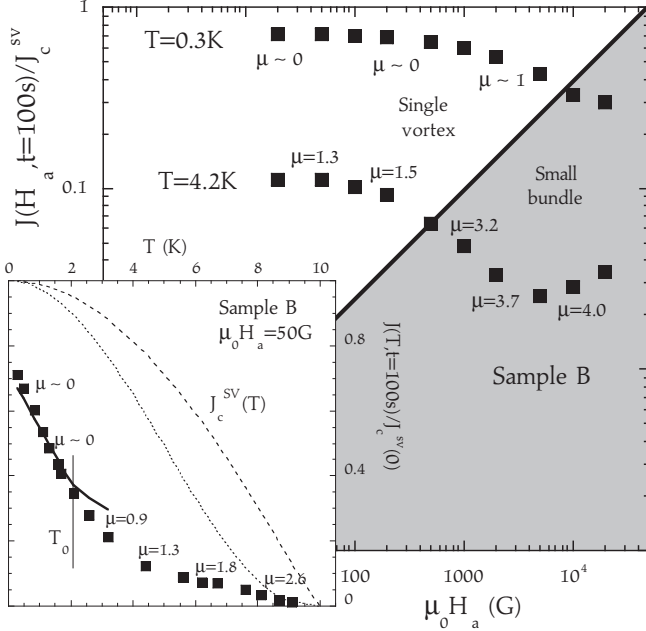


FIG. 5. Main panel: Magnetic field dependence of the current density at $t = 100$ s for the indicated temperatures. The solid line separates the single vortex (1D) from the small bundle (3D) creep regimes. Relaxation exponent (μ) values are indicated for some characteristic fields. Inset: Temperature dependence of the current density at $t = 100$ s and $\mu_0 H_a = 50$ G. The dotted and dashed lines correspond to the temperature dependence of the critical current (single vortex regime) for δl and δT_c pinning, respectively. The solid line correspond to $J_c(T)/[t/t_0]^{R(T)}$ with $t_0 \sim 1 \mu s$ (δl pinning as an example).

an increase of μ (tending toward $\sim 3.5-4$ around 1 T). Finally note that a slight increase of μ has also been observed at 0.3 K but for $\mu_0 H_a \geq 1$ T. Note also that R finally increases at high temperature. This increase has recently been attributed to a crossover from an elastic (positive μ) to a plastic (negative μ) creep regime [20]. However, we did not observe such a change in the sign of μ and the increase of R is rather due to a decrease of the pinning energy in the vicinity of the irreversibility line.

In the collective elastic pinning model, pinning is expected to be of single vortex type until the vortex spacing a_0 reaches the collective pinning length L_c , e.g., for $\mu_0 H_a \leq B_{sb} \sim 5 B_{c2} J_c^{SV}/J_0$ [13]. Taking $J_c^{SV} \sim J(0, t=1s) \sim 2 \times 10^5$ A/cm² $\sim J_0(0)/100$ one obtains $B_{sb} \sim 5$ T (below 4.2 K) in our samples, and the small bundle pinning regime is never reached. J_c is hence expected to remain field independent ($=J_c^{SV}$) over the whole magnetic field range used here. However, as $J(t)$ decreases, the characteristic size of the creeping segment $L(J)$ increases ($L(J) \sim (L_c/\epsilon) \times (J_c^{SV}/J)^{5/7}$ [13]) and a crossover from single vortex (1D) to bundle (3D) creep is then expected to be observed when L reaches a_0 even though $\mu_0 H_a < B_{sb}$. As $L_c \sim 10\xi \sim 150$ Å and $J_c^{SV}/J \sim 10$ in our samples at 4.2 K (see Fig. 5) $L \sim 3000$ Å reaches a_0 for $\mu_0 H_a \sim 300$ G, i.e., for $H_a \sim H_{max}$. μ is hence small (and even ~ 0 for $T < T_0$) in the low field single-vortex creep regime and increases with H_a (and/or T) as $L \rightarrow a_0$, finally tending towards $\sim 3.5-4$ for $L > a_0$. Note that although larger, this

μ value is on the order of the one expected in the small bundle creep regime ($\mu = 5/2$).

IV. CONCLUSION

The current density $J_{sb}(H_a) = J_c^{SV} \times (L_c/\epsilon a_0)^{7/5}$ corresponding to the crossover from single vortex to bundle creep is displayed in Fig. 5 (solid line) together with $J(H_a, t = 100s)$ at $T = 0.3$ K and 4.2 K (Sample B). As shown, a significant decrease in $J(H_a, t = 100s)$ is observed for fields much lower than B_{sb} and $J(t = 100s, H_a)$ even becomes nonmonotonic at 4.2 K. Those dependences are dynamical effects. Indeed, the decrease in $J(H_a, t = 100s)$ at low H_a is a consequence of the increase of the relaxation rate [see Fig. 4(a)] and, in contrast to systems such as MgB₂ [21], the further increase in $J(H_a, t = 100s)$ observed above ~ 1000 G at 4.2 K is not related to any phase transition in the vortex solid but to the slowdown of the relaxation as the system enters the bundle creep regime [22]. Similarly, at low temperature (and low H_a) $\mu \sim 0$ and $J(T, t)$ is expected to vary as $J_c(T)/[t/t_0]^{R(T)}$ with $J_c(T) = J_c^{SV}(T) = J_0(\epsilon \xi_{ab}/L_c)^2$, $J_0(T) \propto 1/\lambda_{ab}^2(T)$, $\xi_{ab}(T) \approx [1 - (T/T_c)^2]^{3/2}$ and $(\epsilon \xi_{ab}/L_c)^2 \approx [1 - (T/T_c)^2]^\alpha$ with an exponent α depending on the microscopic origin of pinning [23]. As shown in the inset of Fig. 5, $J(t, t = 100s)$ strongly differs from $J_c(T)$ for both pinning induced by fluctuations of the mean free path (δl pinning, dotted line) or by fluctuations in the critical temperature (δT_c pinning, dashed line). The strong (\sim exponential) temperature decrease observed for $T \leq T_0 \sim 2$ K is again a dynamical effect related now to the increase of $R(T)$ at low temperature (see solid line in the inset of Fig. 5 with $t_0 \sim 1 \mu s$) and those large creep effects are hence compromising any analysis of the temperature [7] (and/or field) dependence of the critical current in this system. Note that it was not possible to distinguish between δl and δT_c pinning and the solid line in the inset of Fig. 5 corresponds, as an example, to δl pinning ($\alpha = 1$).

In conclusion, we have shown that small activation barriers and a large quantum creep rate are at the origin of a rapid decay of the current density $J(T, H_a, t)$ in Fe_{1+ δ} (Te _{x} Se_{1- x}). The logarithmic relaxation rates remain finite down to $\sim T_c/50$ ($R|_{T \rightarrow 0} \rightarrow 2\%$) suggesting that quantum creep becomes important at low temperature. The relaxation exponent $\mu \rightarrow 0$ at low T and low H_a and $R(T, H)$ first increases with T and/or H_a but then decreases due to a fast increase of μ as the size of the creeping segment $L(J)$ is approaching the vortex spacing a_0 [crossover from single vortex (1D) to bundle (3D) creep].

ACKNOWLEDGMENTS

This work has been supported by the French National Research Agency, Grant No. ANR-09-Blanc-0211 SupraTetrafer. T.K. is most obliged to Z. Pribulova from the Centre of Low Temperature Physics, Slovak Academy of Sciences, Košice, Slovakia and F. Gucman from the Institute of Electrical Engineering, Slovak Academy of Sciences, Bratislava, Slovakia for the development of the Hall sensors used in this study. H.G. thanks the LANEf for financial support.

- [1] Y. Kamihara, T. Watanabe, M. Hirano, and H. Hosono, *J. Am. Chem. Soc.* **130**, 3296 (2008); X. H. Chen, T. Wu, G. Wu, R. H. Liu, H. Chen, and D. F. Fang, *Nature (London)* **453**, 761 (2008).
- [2] F. C. Hsu, J. Y. Luo, K. W. Yeh, T. K. Chen, T. W. Huang, P. M. Wu, Y. C. Lee, Y. L. Huang, Y. Y. Chu, D. C. Yan, and M. K. Wu, *Proc. Natl. Acad. Sci. USA* **105**, 14262 (2008).
- [3] B. C. Sales, A. S. Sefat, M. A. McGuire, R. Y. Jin, D. Mandrus, and Y. Mozharivskyj, *Phys. Rev. B* **79**, 094521 (2009); K.-W. Yeh, T. W. Huang, Y. L. Huang, T. K. Chen, F. C. Hsu, P. M. Wu, Y. C. Lee, Y. Y. Chu, C. L. Chen, J. Y. Luo, D. C. Yan, and M. K. Wu, *Europhys. Lett.* **84**, 37002 (2008); M. H. Fang, H. M. Pham, B. Qian, T. J. Liu, E. K. Vehstedt, Y. Liu, L. Spinu, and Z. Q. Mao, *Phys. Rev. B* **78**, 224503 (2008).
- [4] T. Klein, D. Braithwaite, A. Demuer, W. Knafo, G. Lapertot, C. Marcenat, P. Rodière, I. Sheikin, P. Strobel, A. Sulpice, and P. Toulemonde, *Phys. Rev. B* **82**, 184506 (2010).
- [5] A. Tamai, A. Y. Ganin, E. Rozbicki, J. Bacsá, W. Meevasana, P. D. C. King, M. Caffio, R. Schaub, S. Margadonna, K. Prassides, M. J. Rosseinsky, and F. Baumberger, *Phys. Rev. Lett.* **104**, 097002 (2010).
- [6] A. Serafin, A. I. Coldea, A. Y. Ganin, M. J. Rosseinsky, K. Prassides, D. Vignolles, and A. Carrington, *Phys. Rev. B* **82**, 104514 (2010).
- [7] M. Bonura, E. Giannini, R. Viennois, and C. Senatore, *Phys. Rev. B* **85**, 134532 (2012).
- [8] R. Prozorov, N. Ni, M. A. Tanatar, V. G. Kogan, R. T. Gordon, C. Martin, E. C. Blomberg, P. Prommapan, J. Q. Yan, S. L. Budko, and P. C. Canfield, *Phys. Rev. B* **78**, 224506 (2008); Huan Yang, Cong Ren, Lei Shan, and Hai-Hu Wen, *ibid.* **78**, 092504 (2008); Bing Shen, Peng Cheng, Zhaosheng Wang, Lei Fang, Cong Ren, Lei Shan, and Hai-Hu Wen, *ibid.* **81**, 014503 (2010); M. Konczykowski, C. J. van der Beek, M. A. Tanatar, Huiqian Luo and Zhaosheng Wang, Bing Shen, and Hai Hu Wen, R. Prozorov, *ibid.* **86**, 024515 (2012).
- [9] Y. Yeshurun and A. P. Malozemoff, *Phys. Rev. Lett.* **60**, 2202 (1988); A. P. Malozemoff and M. P. A. Fisher, *Phys. Rev. B* **42**, 6784 (1990); N. Chikumoto, M. Konczykowski, N. Motohira, and A. P. Malozemoff, *Phys. Rev. Lett.* **69**, 1260 (1992).
- [10] L. Fruchter, A. P. Malozemoff, I. A. Campbell, J. Sanchez, M. Konczykowski, R. Griessen, and F. Holtzberg, *Phys. Rev. B* **43**, 8709 (1991); A. V. Mitin, *Zh. Eksp. Teor. Fiz.* **93**, 590 (1987) [*Sov. Phys. JETP* **66**, 335 (1987)]; A. C. Mota, P. Visani, and A. Pollini, *Phys. Rev. B* **37**, 9830 (1988); A. C. Mota, A. Pollini, G. Juri, P. Visani, and B. Hilti, *Physica A* **168**, 298 (1990).
- [11] G. Blatter and V. Geshkenbein, *Phys. Rev. B* **47**, 2725 (1993).
- [12] M. V. Feigelman, V. B. Geshkenbein, A. I. Larkin, and V. M. Vinokur, *Phys. Rev. Lett.* **63**, 2303 (1989).
- [13] G. Blatter, M. V. Feigelman, V. B. Geshkenbein, A. I. Larkin, and V. M. Vinokur, *Rev. Mod. Phys.* **66**, 1125 (1994).
- [14] Y. Abulafia, A. Shaulov, Y. Wolfus, R. Prozorov, L. Burlachkov, Y. Yeshurun, D. Majer, Z. Zeldov, H. Wühl, V. B. Geshkenbein, and V. M. Vinokur, *Phys. Rev. Lett.* **77**, 1596 (1996); T. Klein, W. Harneit, L. Baril, C. Escribe-Filippini, and D. Feinberg, *ibid.* **79**, 3795 (1997).
- [15] P. W. Anderson and Y. B. Kim, *Rev. Mod. Phys.* **36**, 39 (1964).
- [16] E. Zeldov, N. M. Amer, G. Koren, A. Gupta, M. W. McElfresh, and R. J. Gambino, *Appl. Phys. Lett.* **56**, 680 (1990).
- [17] V. M. Vinokur, M. V. Feigelman, and V. B. Geshkenbein, *Phys. Rev. Lett.* **67**, 915 (1991).
- [18] Hechang Lei, Rongwei Hu, E. S. Choi, J. B. Warren, and C. Petrovic, *Phys. Rev. B* **81**, 094518 (2010); M. H. Fang, H. M. Pham, B. Qian, T. J. Liu, E. K. Vehstedt, Y. Liu, L. Spinu, and Z. Q. Mao, *ibid.* **78**, 224503 (2008); T. Gebre, G. Li, J. B. Whalen, B. S. Conner, H. D. Zhou, G. Grissonnanche, M. K. Kostov, A. Gurevich, T. Siegrist, and L. Balicas, *ibid.* **84**, 174517 (2011).
- [19] A. strong T and H dependence of μ has also been reported in high-temperature oxides, see, for instance, T. Klein, W. Harneit, I. Joumard, J. Marcus, C. Escribe-Filippini, and D. Feinberg, *Europhys. Lett.* **42**, 79 (1998) and references in [13].
- [20] Yue Sun, Toshihiro Taen, Yuji Tsuchiya, Sunseng Pyon, Zhixiang Shi and Tsuyoshi Tamegai, *Europhys. Lett.* **103**, 57013 (2013).
- [21] T. Klein, R. Marlaud, C. Marcenat, H. Cercellier, M. Konczykowski, C. J. van der Beek, V. Mosser, H. S. Lee, and S. I. Lee, *Phys. Rev. Lett.* **105**, 047001 (2010) and references therein.
- [22] A. similar effect has been previously reported in YBaCuO by L. Krusin-Elbaum, L. Civale, V. M. Vinokur, and F. Holtzberg, *Phys. Rev. Lett.* **69**, 2280 (1992).
- [23] $\alpha = 1$ for pinning induced by fluctuations of the mean free path and $\alpha = -1/3$ for fluctuations of the critical temperature, see for instance G. P. Mikitik and E. H. Brandt, *Phys. Rev. B* **64**, 184514 (2001).